Simulation of Tracer Concentration Data in the Brush Creek Drainage Flow Using an Integrated Puff Model

K. SHANKAR RAO, RICHARD M. ECKMAN AND RAYFORD P. HOSKER, JR.

Atmospheric Turbulence and Diffusion Division, NOAA/ARL, Oak Ridge, Tennessee

(Manuscript received 17 February 1988, in final form 13 July 1988)

ABSTRACT

During the 1984 ASCOT field study in Brush Creek Valley, two perfluorocarbon tracers were released into the nocturnal drainage flow at two different heights. The resulting surface concentrations were sampled at 90 sites, and vertical concentration profiles at 11 sites. These detailed tracer measurements provide a valuable dataset for developing and testing models of pollutant transport and dispersion in valleys.

In this paper, we present the results of Gaussian puff model simulations of the tracer releases in Brush Creek Valley. The model was modified to account for the restricted lateral dispersion in the valley, and for the gross elevation differences between the release site and the receptors. The variable wind fields needed to transport the puffs were obtained by interpolation between wind profiles measured using tethered balloons at five along-valley sites. Direct turbulence measurements were used to estimate diffusion. Subsidence in the valley flow was included for elevated releases.

Two test simulations—covering different nights, tracers, and release heights—were performed. The predicted hourly concentrations were compared with observations at 51 ground-level locations. At most sites, the predicted and observed concentrations agree within a factor of 2 to 6. For the elevated release simulation, the observed mean concentration is 40 pL/L, the predicted mean is 21 pL/L, the correlation coefficient between the observed and predicted concentrations is 0.24, and the index of agreement is 0.46. For the surface release simulation, the observed mean is 85 pL/L, and the predicted mean is 73 pL/L. The correlation coefficient is 0.23, and the index of agreement is 0.42. The results suggest that this modified puff model can be used as a practical tool for simulating pollutant transport and dispersion in deep valleys.

1. Introduction

In the autumn of 1984, the U.S. Department of Energy's (DOE) Atmospheric Studies in Complex Terrain (ASCOT) program conducted a major field experiment in the Brush Creek Valley of western Colorado. The specific objective of the experiment was to investigate nocturnal drainage flow and diffusion within the valley in order to improve knowledge of the transport and dispersion processes in complex terrain. Many measurement systems, including tethered balloons and towers, were deployed within the valley to obtain wind and temperature profiles and turbulence data in the drainage flow. Two conservative gaseous tracers were released at the same location at two different heights within the drainage layer; a third tracer and smoke were released at another location. These releases took place on five different nights. The concentrations were sampled at 90 ground-level receptors located on four arcs (three across the main valley, and one across a tributary) and along the valley axis. In addition, vertical concentration profiles were measured at 11 sites. These detailed wind and tracer measurements provide a valuable dataset for developing and evaluating models of pollutant transport and dispersion in complex terrain.

Because of the relative simplicity of the drainage flow in the Brush Creek Valley, we selected an integrated Gaussian puff model that uses a two-dimensional wind field and modified it to simulate the Brush Creek tracer data. In this paper, we briefly describe the 1984 ASCOT experiment, the modified puff model, and our simulations of two tracer experiments covering different nights, tracers, and release heights. We present and discuss results of comparisons between the model predictions and observed ground-level concentrations. The paper concludes with some suggestions for future research and model improvements.

2. The 1984 Brush Creek experiment

A detailed description of the 1984 ASCOT field study in Brush Creek Valley, including technical objectives, measurements, and instrumentation, is given by Clements et al. (1989a). Brush Creek Valley (Fig. 1) is a 25 km long canyon located 55 km NNE of Grand Junction in western Colorado. The valley runs from NW to SE, drains into Roan Creek, and has sidewalls

Corresponding author address: Dr. K. Shankar Rao, Atmospheric Turbulence and Diffusion Division, NOAA/ARL, P.O. Box 2456, Oak Ridge, TN 37831.

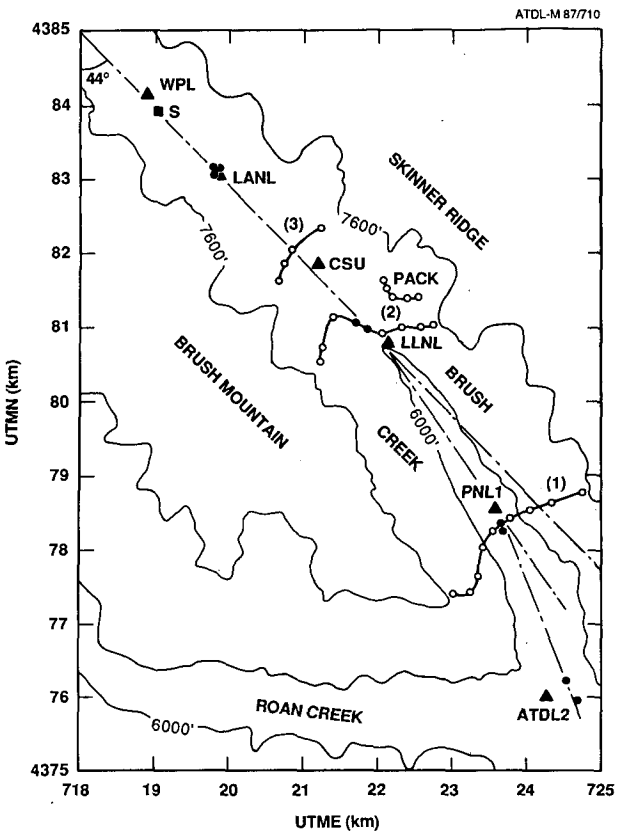

FIG. 1. Brush Creek Valley showing the tracer release site (S) and sampling arcs (1), (2), and (3). Valley-axis samplers are denoted by ●, and tethered-balloon sites by ▲. The arc samplers are indicated by O.

with slopes of 30° to 40°. The floor grade is about 2%, and the valley is 650 m deep at its lower end. The valley has no major tributaries except for a number of short box canyons in the east wall.

During the 1984 experiment, tethered balloon soundings were conducted at several sites in the lowest 10 km length of the valley. The soundings measured the vertical profiles of wind, temperature, and humidity to a height of about 750 m above ground level. Those sites located along the valley axis are shown in Fig. 1. On the experiment nights, data were collected during the balloon ascents at 90 min intervals from 2330 to 1000 MST.

Two gaseous perfluorocarbon tracers, PMCH (PP_2) and PDCH (PP_3), were released at location S (see Fig. 1) at different heights. These tracers were sampled at ground-level sites located on three arcs and along the valley axis, as shown in Fig. 1.

3. Data analysis

The general weather conditions and drainage flow characteristics for the five experiment nights are discussed by Gudiksen and Shearer (1989). We selected two experiment nights, 25/26 September (referred to as Test 2) and 29/30 September (Test 4), for our model simulations, because these nights had well-established drainage flows. Although remotely sensed wind data were obtained with Doppler sodars and a Doppler lidar, we used only the tethered balloon data, as we felt these are more representative of the kind and quality of data likely to be available at a typical site survey. Along-axis tethered balloon soundings for the two experiment nights were checked and interpolated vertically and temporally to obtain profiles of hourly averaged wind and temperature. A linear interpolation between these station profiles was used to develop a wind field for the entire Brush Creek Valley. For the wind field interpolation, the valley was assumed to be trapezoidal in cross section, with its bottom taken as the canyon width at 100 ft above the lowest elevation of the valley floor, and top given by the canyon width at the 7600 ft elevation contour (see Fig. 1). Following the analysis by Clements et al. (1989b), we assumed that the cross-canyon wind distribution is parabolic, with the maximum at the tethered balloon site near the valley axis.

Table 1 gives the source information for the two tracer tests simulated here. These tracers were sampled at 54 ground-level receptors, 25 of which were located on arc 1, 13 on arc 2, and 6 on arc 3; the remaining samplers were distributed along the valley axis. The three arcs were roughly perpendicular to the valley axis, at distances of 7.2 km, 4 km, and 2.5 km, respectively, from the tracer release site. The samplers near the center of each arc were located at the bottom of the approximately bowl-shaped cross section of the valley, while the samplers near the ends of the arc extended up the valley sidewalls to heights ranging from 200 m (for arc 3) to 475 m (for arc 1) above the valley floor. Most of the samplers reported 60 min or 30 min average concentrations; nine sequential samplers reported 15 min averages. All observed concentrations were converted to hourly averaged values for comparison with model predictions. Gudiksen and Shearer (1989) describe the general characteristics of the tracer distributions observed in the 1984 Brush Creek experiments.

4. The model and input data

The integrated puff model (INPUFF-2) described by Petersen and Lavdas (1986) is based on Gaussian

TABLE 1. Summary of tracer release conditions. UTM coordinates of tracer release site S: x = 719.06 km, y = 4383.92 km.

	Test 2	Test 4
Tracer	PDCH (PP_3)	PMCH (PP_2)
Mol.weight (g)	400	350
Date	26 Sep 1984	30 Sep 1984
Release duration (MST)	0000–0900	0030–0800
Avg. release rate (g s^{-1})	0.24	0.23
Release height (m)	180	5

puff assumptions, and is designed to simulate dispersion from point sources utilizing a spatially and temporally variable wind field supplied by the user. This model is capable of using puff-dispersion parameters based on direct turbulence measurements to estimate concentrations at up to 100 receptors. The wind direction is assumed to be constant with height, and only level terrain is considered.

We modified the INPUFF-2 model for tracer simulations in the Brush Creek Valley. Modifications were made to the model to account for the following: (i) differences in elevations of the tracer release site and the samplers in complex terrain, (ii) restricted lateral dispersion of the puffs due to presence of valley sidewalls, (iii) well-mixed lateral and/or vertical dispersion regimes in a deep, narrow valley, and (iv) output concentrations in user-specified units.

The Brush Creek Valley and its environs are represented in the model by a 10 km × 3 km rectangular region with its centerline along the valley axis. The two-dimensional meteorological grid (see Fig. 2), encompassing the five tethered-balloon sites from WPL to PNL1, is taken parallel to the valley floor at the height of tracer emission. The meteorological grid consists of 10 × 10 cells, each with length = 732 m and width = $^1/_{10}$th of the maximum canyon width (B) at the release height. Because the canyon width is larger at the 180 m release height in Test 2 than it is at the 5 m release height in Test 4, the cell width is 128 m in Test 2 and 50 m in Test 4. The down-valley and cross-canyon velocity components, u and v, are specified at the center of each of the grid cells. These velocities are determined at the tracer release height from the spatial and temporal interpolations of the observed wind speeds and directions, as described above.

The restricted lateral dispersion of the puffs in the valley is accounted for by including two image sources or reflections (I_1 and I_2) in the sidewalls for each puff (P); this is schematically illustrated in Fig. 2. Harvey and Hamawi (1986) suggest this approach is most appropriate during stable lapse rate conditions, when the plume centerline can generally be assumed to follow the valley's contours. Thus the contribution of a puff, P, at (x_p, y_p, z_p) to the concentration at a receptor, R, located at (x_r, y_r, z_r) is calculated as follows:

$$C(x_r, y_r, z_r) = \frac{Q}{(2\pi)^{3/2}\sigma_x \sigma_y \sigma_z} g_x(x_r) g_y(y_r) g_z(z_r), \tag{1}$$

where

$$g_x(x_r) = \exp\left\{\frac{-(x_r - x_p)^2}{2\sigma_x{}^2}\right\}, \quad \sigma_x = \sigma_y \tag{1a}$$

$$g_y(y_r) = \exp\left\{\frac{-(y'_r - y'_p)^2}{2\sigma_y{}^2}\right\} + \exp\left\{\frac{-(y'_r + y'_p)^2}{2\sigma_y{}^2}\right\} + \exp\left\{\frac{-[2B - (y'_r + y'_p)]^2}{2\sigma_y{}^2}\right\} \tag{1b}$$

$$g_z(z_r) = \exp\left\{\frac{-(z_r - z_p)^2}{2\sigma_z{}^2}\right\} + \exp\left\{\frac{-(z_r + z_p)^2}{2\sigma_z{}^2}\right\}. \tag{1c}$$

Here Q is the source emission rate (g s^{-1}), and y' is the y-distance measured from the valley sidewall that is the closest to the x-axis (see Fig. 2). The variables z_p and z_r represent the heights of the puff and the receptor, respectively, above the floor of Brush Creek Valley. In order to account for the gross elevation differences between the tracer release site and the various receptor sites, z_r is calculated by subtracting the elevation (MSL) of the tracer release site S from the ele-

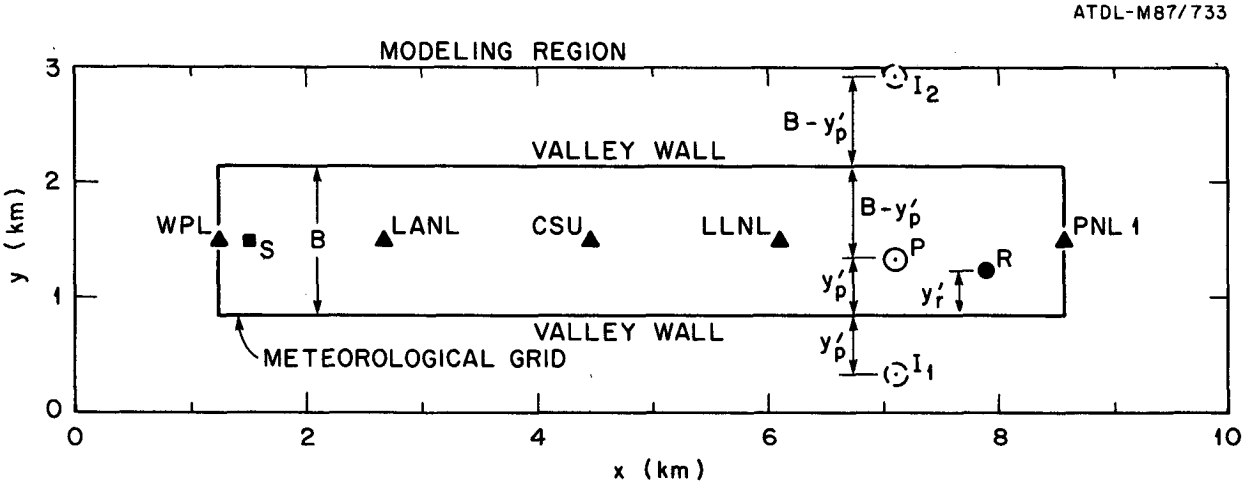

FIG. 2. Modeling region and meteorological grids used in the tracer data simulations, showing the source (S) and Tethersonde sites (▲). A puff (P) and its reflections (I_1 and I_2) in the two sidewalls are shown for the scheme used to account for restricted lateral dispersion in a valley.

vation of each receptor site R, and then adding the 2% grade of the valley floor over the distance $(x_r - x_s)$. The puff trajectory is assumed to be parallel to the valley floor, and so z_p is given by the release height of the neutrally buoyant tracer (see Table 1). The second term in Eq. (1c) represents the contribution of the image of the puff in the valley floor.

For the elevated (183 m AGL) release case (Test 2), unexpectedly high concentrations were observed at the bottom of the valley at some arc 3 and valley-axis receptors near the source. This suggests the occurrence of either a strong subsidence in the upper part of the valley, or a possible surface leak of tracer that could not be accounted for in the simulations. For the night of 25/26 September, Horst et al. (1987) evaluated the thermal energy budgets in the Brush Creek Valley drainage flow, and estimated subsidence rates of up to 9 cm s^{-1} near ridge top, corresponding to a large increase in the valley cross section with down-valley distance. Subsidence would cause the puffs to sink toward the ground from the release height. This was simulated in the model by replacing the release height z_p in Eq. (1c) with $z'_p = z_p - wt$, where w is the assumed average subsidence velocity and t is the puff travel time.

For $\sigma_z > 0.8h$, where h is the mixing depth, the puff is assumed to be well mixed vertically, giving a uniform concentration profile with height (Turner 1974). In this case, the concentration is calculated from Eq. (1) with

$$g_z(z_r) = 2, \quad \sigma_z = 0.8h. \tag{2}$$

Similarly, for $\sigma_y > 0.8B$, the puff is assumed to be laterally well mixed, and the concentration is calculated from Eq. (1) with

$$g_y(y_r) = 2, \quad \sigma_y = 0.8B. \tag{3}$$

If the puff is well mixed both laterally and vertically, the concentration is calculated from Eq. (1) after substituting Eqs. (2) and (3).

The mixing depth in Brush Creek Valley, taken to be the depth of the drainage flow, is determined from the vertical profiles of wind speed and direction. The top of the drainage layer is generally characterized by a near-zero wind speed and a sharp discontinuity in the wind direction. Hourly values of drainage flow depth determined from the soundings at the five tethered balloon sites shown in Fig. 2 were averaged to obtain mixing depths for Brush Creek Valley. These values ranged from 313 to 431 m for Test 2 and 419 to 469 m for Test 4, during the simulation period (0000–1000 MST).

As described by Petersen (1986), INPUFF-2 includes an option for estimating σ_y and σ_z from the measured standard deviations of horizontal and vertical wind direction fluctuations (σ_θ and σ_ϕ). This option uses the dispersion schemes summarized by Irwin (1983). The use of direct measurements of turbulence to estimate dispersion parameters was recommended by an American Meteorological Society workshop (Hanna et al. 1977).

Hanna (1981) showed that values of σ_θ in complex terrain during nighttime stable conditions are generally enhanced over those measured or predicted by similarity theory over flat terrain. He found that the average observed σ_θ at a height of 10 m at 11 stations in the nocturnal drainage flow in Anderson Creek Valley in California was about 25°, close to the value predicted by similarity theory for neutral thermal stability. Gudiksen (1989) analyzed the hourly averaged σ_θ values observed at three surface stations in the drainage flows of both the Anderson and Brush Creek valleys. These values ranged over two orders of magnitude, from a few degrees to a little over 100°, with the median values between 15° and 40°. Stations situated on the valley floor and along the lower slopes showed the highest median values, while the ridge stations gave the lowest values.

During the 1984 Brush Creek experiment, Doppler acoustic sounders, towers, and a turbulence probe mounted on a tethered balloon were used to measure σ_θ (or σ_v) and σ_w at several sites and heights in the valley. The locations of these sites and a description of the measurements can be found in Clements et al. (1989a). These turbulence data, analyzed by Rao and Schaub (1989) for the two nights of the present simulations, give results which are consistent with the earlier work described above. For the period 2300–0600 MST, the hourly average observed values of σ_θ and σ_ϕ in the nocturnal drainage flows are about 20°–25° and 5°, respectively. After sunrise, as the surface warms and the flow direction reverses (up-valley flow), these parameters increase sharply to their maximum values at 0800 MST, which approximately corresponds to the time of occurrence of sunshine on the valley floor. By 1000 MST, σ_θ and σ_ϕ decrease to their normal daytime values. There is general agreement between the variations of the hourly average σ values determined from the sodar data and the tower data. These observed σ_θ and σ_ϕ values were used to specify σ_y and σ_z in the puff-model simulations of the tracer data.

An option was added to the model to convert the calculated concentrations from g m^{-3} to any user-specified units. In the present simulations, this option was used to calculate concentrations in picoliters/liter (1 pL/L = 10^{-12} liters/liter) for comparison with the observed concentrations.

5. Results and discussion

Hourly concentrations from 0000–1000 MST for Test 2 and Test 4 were computed at 51 surface samplers on the three arcs and along the valley axis; the remaining 3 valley samplers were outside the model domain. The model simulations were evaluated by comparing the calculated hourly concentrations at each sampler with the corresponding observed values.

Table 2 shows the evaluation statistics for the two simulations. The statistics are those discussed by Fox (1981) and Rao et al. (1985). For the elevated release case (Test 2), the mean of the concentrations observed at all 51 receptors, $\bar{O}$, is 40 pL/L while the mean of the predicted concentrations, $\bar{P}$, is 21 pL/L. The corresponding results for the surface release case (Test 4) are 85 pL/L and 73 pL/L, respectively. These results indicate that the simulations for the surface release case are generally better, though the correlation coefficients (0.24 and 0.23) and the indices of agreement (0.46 and 0.42) are nearly the same for the two cases.

The observed data show large spatial and temporal variability. The ratio of the standard deviation to the mean of the observations is large—about 1.4 for both tests. The corresponding values of this ratio for the predictions is about 1.0 for Test 2 and 0.8 for Test 4. Extremely small (near-zero) values of concentrations were measured at some stations; about 23% of the observed concentrations for Test 2 (21% for Test 4) are smaller than 1 pL/L. Excluding $O_i < 1$ pL/L from comparisons, the mean of the ratios (P_i/O_i) is 2.3 for Test 2 and 5.7 for Test 4. Both tests show a significantly larger fraction of the mean squared error attributable to systematic errors; this suggests there is room for improvement of the model simulations, for example, by a better representation of the effects of the terrain on the transport wind field.

The statistics for restricted time intervals and individual arcs were also calculated, but are not shown here. The simulations are generally better for 0000–0500 MST period for the elevated release, and for the 0600–1000 MST period for the surface release. During the latter period, the stability conditions were slightly convective following local sunrise (after about 0600 MST). The nocturnal drainage flow weakened during this morning transition period, giving way to upslope flows along the heated western sidewall that led to the ventilation of the tracers out of the valley. For both tests, the results for the entire simulation period are better at arc 1, which has the most samplers and is located farthest from the source, than at other receptors within the valley. At arc 1 for Test 2, $\bar{O} = 21.4$ pL/L, $\bar{P} = 21.6$ pL/L, and $R = 0.61$; for Test 4, $\bar{O} = 45.4$ pL/L, $\bar{P} = 49.2$ pL/L, and $R = 0.29$. This suggests that the model performs better far from the source, where the model's assumption of a well-mixed puff is more appropriate, especially for an elevated release.

Figure 3a presents a comparison of the predicted and observed hourly concentrations for Test 2, averaged over all sampling stations. The results show that the concentrations from the elevated release (Test 2), on the average, are underpredicted over the most of the simulation period. Figures 3b and 3c show similar comparisons for the receptors in arc 1 and arc 2, respectively. Though the trends in the observed concentrations are tracked fairly well at both arcs, the simulations at arc 1 are much better, as noted before. The corresponding plots for the surface release (Test 4) are presented in Fig. 4a–c. The results suggest that the average observed concentrations are simulated fairly well over all samplers and at arc 1, except for the first 3 hours of the simulation period. Though the model cannot explicitly account for the heating or shading of the valley sidewalls after sunrise, it is encouraging that the observed average concentrations during the morning transition period (after 0600 MST) are tracked fairly well in both tests.

Figures 5a and 5b show frequency plots for all the hourly averaged concentrations in Test 2 and Test 4, respectively. This type of plot will often have a bimodal distribution because some of the receptors will usually be outside the plume (producing the lower mode), while some of the receptors inside the plume will be

TABLE 2. Evaluation statistics for model simulations. S.D. = standard deviation, RMSE = root-mean-square error, R = correlation coefficient. The index of agreement is defined as $d = 1 - \{\sum (O_i - P_i)^2 / \sum [|P_i - \bar{O}| + |O_i - \bar{O}|]^2\}$. The unsystematic and systematic parts of the mean square error (MSE) are: $\text{MSE}(u) = (1/N) \sum (P_i - \hat{P}_i)^2$, $\text{MSE}(s) = (1/N) \sum (\hat{P}_i - O_i)^2$, where $\hat{P}_i$ is the estimate of the predicted concentration given by $\hat{P}_i = a + bO_i$. All sums are for $i = 1, 2, \cdots, N$, where N is the number of observations.

	Test 2		Test 4	
	Obs. (O)	Pred. (P)	Obs. (O)	Pred. (P)
Mean ($\bar{O}$ and $\bar{P}$; pL/L)	40.4	21.4	84.8	72.6
S.D. (pL/L)	57.4	22.2	120.0	56.2
Range of O_i (pL/L)	0–307		0–509	
No. of Samples (N)	307		243	
R	0.24		0.23	
Slope (b)	0.10		0.11	
Intercept (a; pL/L)	17.6		63.6	
Bias (pL/L)	19.0		12.1	
RMSE (pL/L)	59.4		121.0	
Index of Agreement (d)	0.46		0.42	
MSE(u)/MSE	13%		20%	
MSE(s)/MSE	87%		80%	

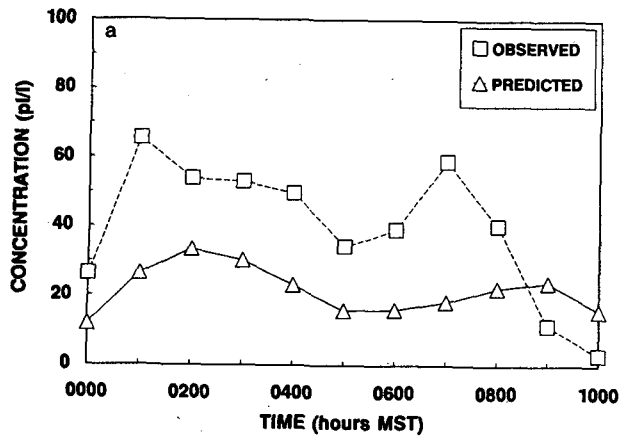

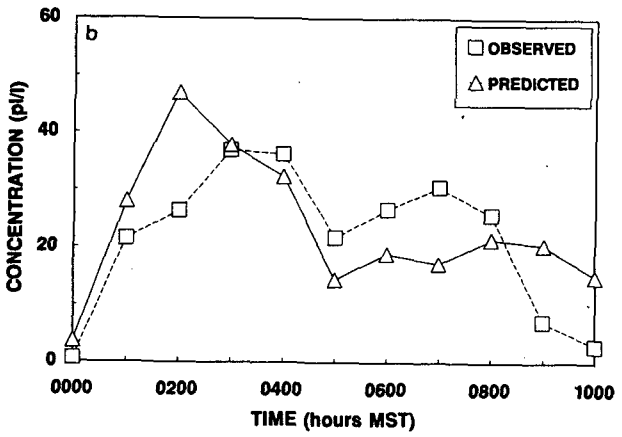

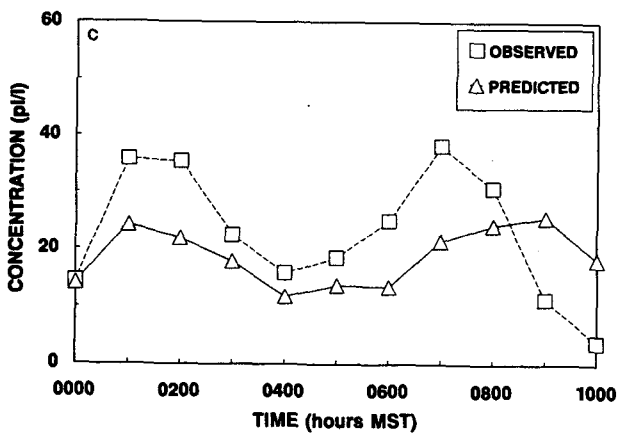

FIG. 3. Comparison of predicted and observed hourly PP_3 tracer (Test 2) concentrations, averaged over the samplers, for the simulation period 0000–1000 MST. The times shown in the figure denote the beginning of each hourly sampling period; (a) for all 51 samplers, (b) for arc 1 samplers only, and (c) for arc 2 samplers only.

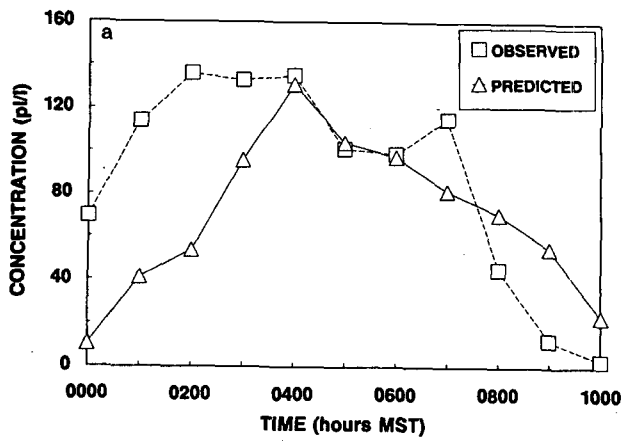

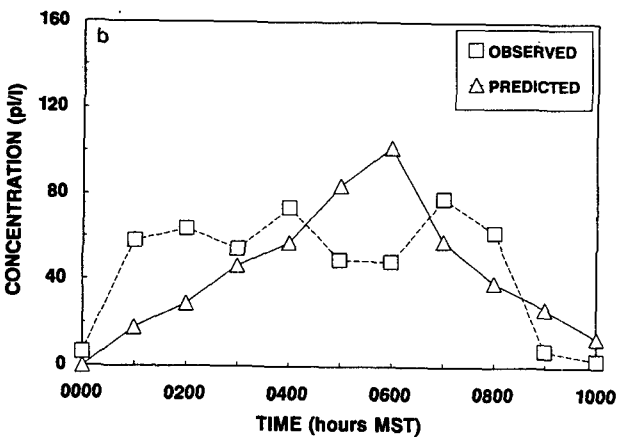

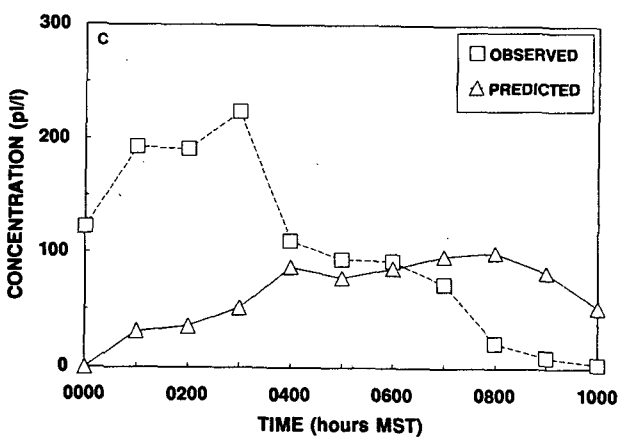

FIG. 4. Comparison of predicted and observed hourly PP_2 tracer (Test 4) concentrations, averaged over the samplers, for the simulation period 0000–1000 hrs MST. The times shown in the figure denote the beginning of each hourly sampling period; (a) for all 51 samplers, (b) for arc 1 samplers only, and (c) for arc 2 samplers only.

close to the plume centerline (producing the upper mode). Both the observed and predicted frequencies, shown in Fig. 5a and 5b, approximate a bimodal distribution. The lower peaks are in the first class interval, which includes concentrations between 0 and 1 pL/L. The upper peaks are roughly in the 16–32 pL/L class interval for Test 2 and the 64–128 pL/L class interval for Test 4. The distribution of concentration about each peak is narrower for the predictions than it is for the observations. We interpret this difference as the result

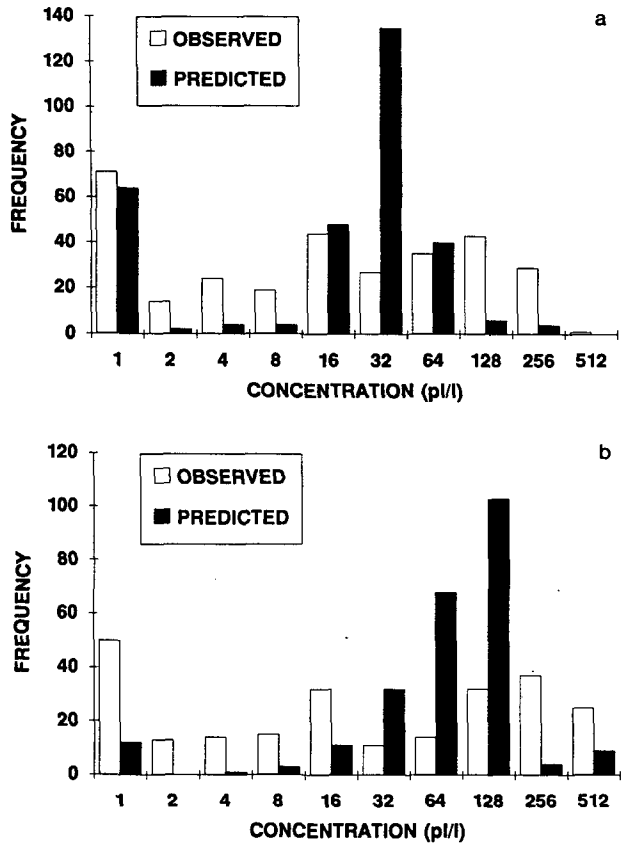

FIG. 5. Frequency plots for all the hour-averaged concentrations from the 51 receptors. The number under each class interval is the upper end of the concentration interval; the lower end of each interval is given by the number under the preceding class interval. For the first class interval, the lower end is 0 pL/L. The ordinate gives the number of observations or predictions in each class interval; (a) for elevated release (Test 2), and (b) for surface release (Test 4).

of limited temporal and spatial resolution in the puff model simulation; the model cannot account for the detailed features of topography and winds which could have affected the concentrations at some receptors. These small-scale local features generally tend to spread the observed concentrations over a greater range than the model predictions.

6. Conclusions

An integrated Gaussian puff model, capable of utilizing a spatially and temporally variable wind field and user-specified dispersion parameters, has been modified to simulate the ground-level tracer concentrations observed at 51 receptors in the Brush Creek Valley drainage flow. Simulations were performed for one elevated release and one surface release, with each release occurring on a different night. At many of the receptors, the predicted and observed hourly averaged concentrations agree to within factors of 2 to 6. The evaluation statistics of the simulations are similar for both the elevated release and surface release cases. The modified puff model may provide an inexpensive alternative to complicated three-dimensional numerical grid models for the simulation of pollutant transport and dispersion in valley environments.

The mean wind transport plays a dominant role in the estimation of pollutant concentrations in complex terrain. It can be argued that the Brush Creek Valley drainage flow represents a relatively simple case of flow over complex terrain, because the flow direction is well defined and the flow structure is understood fairly well. In addition, the plume is confined within the valley because of the steep valley sidewalls, which also tend to isolate the nocturnal drainage flow in the valley from the external flow. This suggests that puff-trajectory models, such as the one described here, should do as well in simulating the dispersion in similar applications elsewhere.

The mechanisms of subsidence and entrainment in valley drainage flows need to be studied further. With present instrumentation, it is difficult to measure accurately the small vertical velocities associated with subsidence in the flow. The numerical analysis of diffusion in two-dimensional katabatic flows performed by Nappo et al. (1989) shows that elevated plume material can be brought down to the ground surface as the turbulent kinetic energy of the flow increases downslope. If this effect is not taken into account, the model concentrations will tend to be underpredicted.

Accounting for the presence of the two sidewalls and the floor of the valley with three image puffs is a reasonable first approximation which is consistent with our model assumption of a trapezoidal cross section for the valley. In reality, a continuous distribution of images may be needed to adequately represent the reflecting boundary condition along the bowl-shaped cross section of the valley. Such complex schemes, currently under development, may lead to higher estimates of the concentrations than are given by the present model.

According to Dobosy et al. (1989), the spatial and temporal variability of the winds and mass balance in Brush Creek Valley cannot be adequately described by a limited number of tethered balloon profile measurements. The decision to use only these data here was dictated by our desire to keep the model simple for practical applications. Though we have derived a three-dimensional wind field from available data, the model uses winds in only a single horizontal plane—generally at the effective source height. In a more detailed model, it would be highly desirable to include vertical shear of wind speed and direction to account for the effects of subsidence and differential cooling and heating of valley sidewalls on the trajectory and shape of the puffs.

Acknowledgments. This work was performed under an agreement between the National Oceanic and At-

mospheric Administration and the U.S. Department of Energy as part of the ASCOT program. The authors acknowledge the assistance of Mr. Karlos Zvonarek, Oak Ridge Associated Universities Summer Research Participant at ATDD in 1986, in the tethered balloon data analysis.

REFERENCES

Clements, W. E., J. A. Archuleta and P. H. Gudiksen, 1989a: Experimental design of the 1984 ASCOT field study. *J. Appl. Meteor.*, **28,** 405–413.

——, —— and D. E. Hoard, 1989b: Mean structure of the nocturnal drainage flow in a deep valley. *J. Appl. Meteor.*, **28,** 457–462.

Dobosy, R. J., K. S. Rao, J. W. Przybylowicz, R. M. Eckman and R. P. Hosker, 1989: Mass and momentum balance in the Brush Creek drainage flow determined from single-profile data. *J. Appl. Meteor.*, **28,** 467–476.

Fox, D. G., 1981: Judging air quality model performance. *Bull. Amer. Meteor. Soc.*, **62,** 599–609.

Gudiksen, P. H., 1989: Categorization of nocturnal drainage flows within the Brush Creek Valley and the variability of sigma theta in complex terrain. *J. Appl. Meteor.*, **28,** 489–495.

——, and D. L. Shearer, 1989: The dispersion of atmospheric tracers in nocturnal drainage flows. *J. Appl. Meteor.*, **28,** 602–608.

Hanna, S. R., 1981: Diurnal variation of horizontal wind direction fluctuations in complex terrain at Geysers, Cal. *Bound.-Layer Meteor.*, **21,** 207–213.

——, G. A. Briggs, J. Deardorff, F. A. Gifford and F. Pasquill, 1977: AMS workshop on stability classification schemes and sigma curves—Summary of recommendations. *Bull. Amer. Meteor. Soc.*, **58,** 1305–1309.

Harvey, R. B., and J. N. Hamawi, 1986: A modification of the Gaussian dispersion equation to accomodate restricted lateral dispersion in deep river valleys. *J. Air Pollut. Control Assoc.*, **36,** 171–173.

Horst, T. W., K. J. Allwine and C. D. Whiteman, 1987: A thermal energy budget for nocturnal drainage flow in a simple valley. Preprints, *Fourth Conference on Mountain Meteorology,* Seattle, Amer. Meteor. Soc., 15–19.

Irwin, J. S., 1983: Estimating plume dispersion—a comparison of several sigma schemes. *J. Climate Appl. Meteor.*, **22,** 92–114.

Nappo, C. J., K. S. Rao and J. A. Herwehe, 1989: Pollutant transport and diffusion in katabatic flows. *J. Appl. Meteor.*, **28,** 617–625.

Petersen, W. B., 1986: A demonstration of INPUFF with the MATS data base. *Atmos. Environ.*, **20,** 1341–1346.

——, and L. G. Lavdas, 1986: INPUFF 2.0—A Multiple Source Gaussian Plume Dispersion Algorithm. EPA-600/8-86-011, U.S. Environmental Protection Agency, Research Triangle Park, NC, 105 pp.

Rao, K. S., and M. A. Schaub, 1989: Observed variations of σ_θ and σ_ϕ in the Brush Creek drainage flow. No. 8131, ATDL Report, NOAA, Oak Ridge, TN, 39 pp.

Rao, S. T., G. Sistala, V. Pagnotti, W. B. Petersen, J. S. Irwin and D. B. Turner, 1985: Evaluation of the performance of RAM with the Regional Air Pollution Study data base. *Atmos. Environ.*, **19,** 229–245.

Turner, D. B., 1974: Workbook of atmospheric dispersion estimates. AP-26, U.S. Environmental Protection Agency, Research Triangle Park, NC, 84 pp.